Honors Capstone Projects and Theses   Honors College

5-6-2020

Comparison of Singular Value Decomposition and Ensemble Empirical Mode Decomposition with Independent Component Analysis for Single-Lead Fetal ECG Extraction

Elizabeth D. Staley

Koen Flores

Tadesse Ghirmai

Follow this and additional works at: https://louis.uah.edu/honors-capstones

Comparison of Singular Value Decomposition and Ensemble Empirical Mode Decomposition with Independent Component Analysis for Single-Lead Fetal ECG Extraction

by

Elizabeth D. Staley[1], Koen Flores[2], and Tadesse Ghirmai Ph.D.[3]

[1]The University of Alabama in Huntsville, [2]University of Florida, [3]University of Washington Bothell

An Honors Capstone
submitted in partial fulfillment of the requirements
for the Honors Diploma
to

The Honors College

of

The University of Alabama in Huntsville

May 6, 2020

Honors Capstone Director: Dr. Emil Jovanov
Associate Professor of Electrical and Computer Engineering

_____   05/06/2020_____
Student   Date

_____   05/06/2020_____
Director   Date

_____   _____
Department Chair   Date

_____   _____
Honors College Dean   Date

Honors College
Frank Franz Hall
+1 (256) 824-6450 (voice)
+1 (256) 824-7339 (fax)
honors@uah.edu

HONORS COLLEGE

THE UNIVERSITY OF ALABAMA IN HUNTSVILLE

Honors Thesis Copyright Permission

This form must be signed by the student and submitted as a bound part of the thesis.

In presenting this thesis in partial fulfillment of the requirements for Honors Diploma or Certificate from The University of Alabama in Huntsville, I agree that the Library of this University shall make it freely available for inspection. I further agree that permission for extensive copying for scholarly purposes may be granted by my advisor or, in his/her absence, by the Chair of the Department, Director of the Program, or the Dean of the Honors College. It is also understood that due recognition shall be given to me and to The University of Alabama in Huntsville in any scholarly use which may be made of any material in this thesis.

Elizabeth D Staley
_____
Student Name (printed)

_____
Student Signature

05/06/2020
_____
Date

Table of Contents

Acknowledgements:

Abstract

The health of a fetus can be monitored using fetal electrocardiogram (fECG). However, low signal to noise ratios complicate the extraction of fECG from abdominal electrocardiogram (aECG), which contains the pregnant mother's electrocardiogram (mECG), the fECG, and noise artifacts. Modern methods utilize multi-lead systems to alleviate the difficulty of blindly separating fECG from aECG, but single-lead systems offer the advantages of minimizing the number of required components and decreasing patient discomfort. In this study, we implement and compare single-lead extraction methods of singular value decomposition (SVD) and empirical mode decomposition with independent component analysis (EEMD-ICA). Using a synthetic aECG, the two methods were compared on peak detection accuracy, signal morphology, and computational efficiency. We found that SVD extracted fECG with less noise and a shorter run time while EEMD-ICA had a higher peak detection accuracy. However, application of SVD and EEMD-ICA on a real aECG suggested that SVD may be more effective than EEMD-ICA at cleanly and completely extracting fECG. Continuation of this work to further improve each extraction method and include more real aECG signals could validate the potential of single-channel fECG extraction for future medical devices.

I. Introduction

Fetal electrocardiogram (fECG) provides important information regarding the cardiovascular health of the fetus. Long-term monitoring of fECG allows for early identification of heart problems such as fetal asphyxia and can reduce infant mortality and morbidity [1]. Low signal to noise ratio (SNR) of fECG to maternal ECG (mECG) and noise complicates fECG extraction from abdominal ECG (aECG). Most existing fECG extraction methods use multiple-channel recordings or fetal scalp electrodes to improve fECG recovery. Widrow *et al*. proposed a multiple-channel adaptive noise cancellation technique that utilizes maternal chest leads as references to extract the fECG from the aECG [2]. However, this technique cannot be constantly administered due to the large number of components and set-up difficulty. Similarly, fetal scalp electrodes suffer the same administration issue because they are only used during delivery. Fetal scalp electrodes have further been associated with increased risk of infection, cuts, and neonatal morbidity [1, 3]. Recent statistical domain decomposition methods aim to address the administration issues of current fECG extraction methods by processing signals from a non-invasive, single lead system. Two such prominently reported extraction methods are Kanjilal *et al*.'s singular value decomposition (SVD) [4] and Mijovic *et al*.'s ensemble empirical mode decomposition with independent component analysis (EEMD-ICA) [5]. In this work, we implement and compare these two methods in terms of their extraction quality and computational efficiency under varying fetal SNRs.

This paper is organized as follows. Section II provides background information and summaries of Kanjilal *et al.*'s and Mijovic *et al.*'s approaches to SVD and EEMD-ICA, respectively. Section III then discusses our implementations of SVD and EEMD-ICA. Section IV introduces the composition of synthetic aECG for testing SVD and EEMD-ICA. The specific

metrics used for comparison of extraction quality and computational efficiency are located in

section V. Section VI presents the results from testing SVD and EEMD-ICA with the metrics

from section V and provides basic comparison of the two methods. Section VII further explores

the effectiveness of SVD and EEMD-ICA by analyzing their ability to extract fECG from a real

aECG. Section VIII then presents an overall discussion and comparison of SVD and EEMD-ICA

and is followed by the conclusion in section IX. Finally, previous versions of this research and

individual author contributions are detailed in the Appendices A and B, respectively.

II. Background

The following section provides an overview of the SVD and EEMD-ICA extraction techniques by first reviewing the theoretical background and then presenting the implementation methods proposed by Kanjilal *et al.* and Mijovic *et al.*, respectively. For EEMD-ICA, the subprocesses of EMD and ICA are introduced before the overall method is considered.

Singular Value Decomposition (SVD)

SVD is a linear-algebra based approach that decomposes signals into orthogonal components. It states that an *mxn* matrix A can be factored into three matrices:

$$A = U\Sigma V^T = \sum_{i=1}^{q} u_i \sigma_i v_i^T \quad (1)$$

where *U* is an orthonormal real *mxm* matrix, *V* is an orthonormal real *nxn* matrix, Σ is a non-negative diagonal matrix with descending singular values (σ), u_i is column *i* of *U*, and v_i is column *i* of *V*. *U* describes the left singular vectors and column space of *A*, and *V* describes the right singular vectors and row space of *A* [4].

Because the singular values are arranged in descending order of importance, the majority of important signal information is contained in the first dyad $u_1 \sigma_1 v_1^T$ if $\sigma_1^2/\sigma_2^2 >> 1$. This property has particularly significant implications for periodic signals. A matrix can be composed from periodic signals by defining the matrix rows as one ECG period. If the signal is strictly periodic, all singular values except σ_1 will equal zero. As the periodicity of the signal declines, the prominence of σ_1 and value of σ_1^2/σ_2^2 also declines. More than one singular value will be large when more than one periodic signal is present in a signal [4]. ECG signals are periodic in nature as a sequence of PQRST waves, so the ability of SVD to identify periodic patterns makes it an optimal fECG extraction method.

Kanjilal *et al*. apply SVD to fECG extraction using the method described below [4] and shown pictorially in Fig. 1:

1) Preprocess the signal to remove low-frequency interference

2) Arrange the filtered aECG into R-peak aligned *mxn* matrix A using a form of interpolation, where *m* is the number of periods in an ECG signal and *n* is the average period length

3) Perform SVD on matrix *A* to obtain the dominant mECG component of the aECG

4) Subtract the extracted mECG from the filtered aECG

5) Repeat steps 2 and 3 to obtain the dominant fECG component
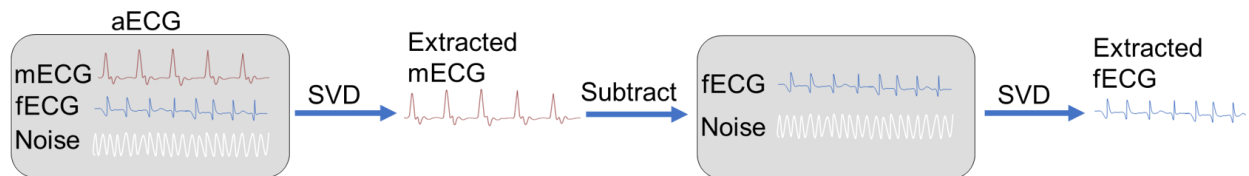
Fig. 1. SVD fECG extraction process

Kanjilal *et al*. describe the general process of their method but do not provide details on how they located R-peaks or interpolated ECG to form the matrices. The discussion of SVD implementation in section III will focus on the development of these algorithms.

Empirical Mode Decomposition (EMD)

EMD is a signal processing method that decomposes nonlinear and non-stationary data into a set of spectrally independent oscillatory modes, known as intrinsic-mode functions (IMFs). EMD decomposes a complicated signal $x(t)$ into a sum of n IMF components $\{c_j(t), j = 1, 2, …, n\}$ and a residual signal $r_n(t)$ as follows:

$$x(t) = \sum_{j=1}^{n} c_j(t) + r_n(t) \qquad (2)$$

EMD does not require prior knowledge about the signal of interest [6]. Common issues with EMD include sensitivity to noise and the mode mixing effect, which introduces additional, fictitious IMFs [7]. To alleviate this issue, a whitening and iterative process of EMD called Ensemble Empirical Mode Decomposition (EEMD) is used [8]. Whitening of the original signal is performed by adding independent and identically distributed white noise with zero-mean and standard deviation (SD) equal to the original SD multiplied by a noise parameter (np). The np is defined as the ratio of noise SD to original SD. EMD is then applied to the whitened signal to derive a set of IMFs. The whitening and selection process are repeated a number of times to yield an ensemble of IMF sets that are then averaged to obtain one final set of IMFs [5].

Independent Component Analysis (ICA)

ICA is a blind signal separation technique that separates multiple observed signals into their independent component sources. In practice, this is done by assuming the observed mixed signals, X, tend towards a Gaussian distribution via the Central Limit Theorem and by maximizing the independence of the estimated sources, S. As opposed to SVD, the estimated independent components (ICs) are not necessarily orthogonal. In addition, ICA estimates the mixing matrix M, such that $X = MS$. Various ICA algorithms attempt to maximize source independence by optimizing features such as negentropy, kurtosis, information transfer, and mutual information [9]. Some existing ICA algorithms include JADE, InfoMax and FastICA [5]. Here, we used the iterative FastICA algorithm to optimize negentropy and calculate the ICs [10]. Once the ICs and mixing matrix are calculated, an IC of interest is multiplied with the mixing matrix to generate the IMF set containing only the component of interest. This IMF set is then summed to obtain the reconstructed signal [5].

Ensemble Empirical Mode Decomposition with Independent Component Analysis (EEMD-ICA)

ICA is ideal for blindly separating signals, but it cannot separate single-source signals such as the aECG examined in this study. This limitation is resolved by combining EMD with ICA, creating a technique called EEMD-ICA. EEMD-ICA first uses EMD to decompose a signal into IMFs. The IMFs are then extracted into statistically independent components using ICA from which the signal of interest can be reconstructed. Mijovic *et al.* demonstrated the effectiveness of EEMD-ICA at identifying epileptic activity and ECG artifacts by extracting a stationary oscillatory signal and a spiky signal from background noise. Mijovic *et al.* found that compared to existing algorithms such as single-channel ICA or wavelet-ICA, EEMD-ICA provided better signal recovery. [5]. However, the study by Mijovic *et al.* did not explore the extraction of a signal from a combined signal with similar components.

<div align="center">**III. Implementations**</div>

Using MATLAB, SVD and EEMD-ICA methods were implemented to extract the fECG component from an aECG. The SVD method extracted the dominant signals of mECG followed by fECG using primary singular values [4]. The EEMD-ICA method extracted the fECG with ICA after repetitions of EMD to obtain multiple observed signals [5].

Singular Value Decomposition (SVD)

A. Preprocessing

Using Kanjilal *et al.*'s method as a guideline, we developed a SVD fECG extraction technique in MATLAB. Prior to performing SVD, the aECG is preprocessed in MATLAB to remove power line interference and baseline wander. MATLAB's iirnotch filter is a type of digital band-stop filter that attenuates a narrow bandwidth of frequencies. This property makes a notch filter ideal to eliminate power line interference because it will not affect signal components with frequencies outside the designated bandwidth. A notch filter with a bandwidth of 5 Hz was thus applied to the aECG to remove 50 Hz power line interference, as found in real aECG signals from the noninvasive fetal ECG PhysioNet database [11]. Additionally, baseline wander was removed using a bidirectional Butterworth high pass filter with a 0.1-10 Hertz stopband. The bidirectional aspect of the filter prevents phase shifting of the aECG [12]. The filtered aECG was then downsampled by a factor of eight to reduce the number of samples contained between two R-peaks (RR period) and manage the SVD input matrix size.

B. Peak Location

In order to compose a SVD input matrix with rows of one PQRST wave, the R-peaks must first be located. Potential R-peaks are located using the MATLAB function *findpeaks* and thresholds *MinPeakHeight*, *MinPeakProminence*, and *MinPeakDistance*. *MinPeakHeight*

measures the amplitude of a signal from the x-axis while *MinPeakProminence* measures the distance to the closest valley of a peak. *MinPeakDistance* ensures identified peaks are separated by a specified distance on the x-axis. Initially, the approximate R-peak amplitude (pMax) is estimated as a fraction of the maximum ECG amplitude to allow for amplitude variation. In our tests, the fraction was selected as 0.6 using trial and error. To account for outliers, the value of pMax was continually reduced until *findpeaks* with a *MinPeakHeight* requirement of the fractioned pMax returned at least the number of expected peaks. The number of expected peaks differed in value depending on the type of signal (i.e. mECG or fECG) analyzed. During mECG extraction, at least 60 peaks for a one-minute length mECG should be found. Similarly, fECG extraction required 100 peaks for a one-minute recording to be found. These values were selected to satisfy minimum standard maternal and fetal heart rates.

Peaks were then reidentified using *findpeaks* with increased and additional thresholds of *MinPeakHeight*, *MinPeakProminence*, and *MinPeakDistance*. The threshold of *MinPeakProminence* prevented the identification of large amplitude noise artifacts as peaks. The specific value of 0.7 for both the peak height and prominence thresholds was determined using trial and error. The value of 0.3 seconds for *MinPeakDistance* was based on the fetal heart rate range from 120 to 160 beats per minute [12]. Conversion of the fetal heart rate range to seconds provides an estimated RR period of 0.375 to 0.5 seconds. The RR period length requirement was thus rounded down to 0.3 seconds, which tolerates abnormal, raised heart rates below 200 bpm. *MinPeakDistance* reduces the identification of nearby, false peaks, but it does not identify missed, low amplitude peaks when the distance between identified peaks is greater than the maximum allowed RR period. Missing peaks were located by reducing the *findpeaks* thresholds

on intervals between identified peaks that were one and a half times greater than the minimum identified RR period.

C. SVD Matrix Formation

Once all peaks were located, the input matrix for SVD was formed by concatenating rows of individual, adjacent ECG periods. To maximize periodicity, the R-peaks were aligned in the same column (see Fig. 2). However, the RR periods were not necessarily the same length. Therefore, a matrix alignment method was required to standardize the length of each row to the average distance between the identified R-peaks (average period). The two matrix alignment techniques implemented were sample duplication and interpolation.
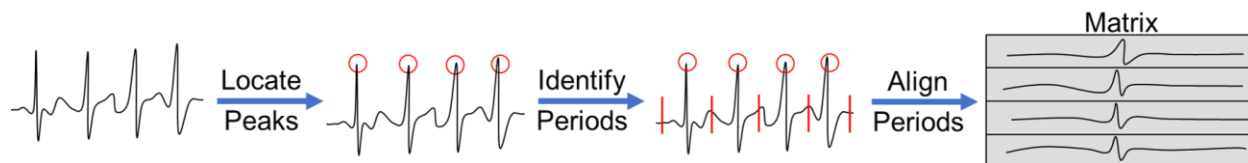

Fig. 2. Matrix Formation of SVD

<u>Sample Duplication</u>

In the sample duplication technique, matrix rows were created by including half of the average period number of samples to both the left and right of the R-peak. If the average period was even, the number of samples included to the left of the R-peak was one less than half the average period, and the number of samples from the right of the R-peak was equal to half the average period. If the average period was odd, the number of samples included to both the left and right of the R-peak was one less than the rounded result of half the average period.

Because this technique does not affect the total number of samples in the original signal, samples may be duplicated in adjacent periods when a period is shorter than the average period. In a drastic case, a P-wave appears at the end of the former ECG period or a T-wave appears at

the beginning of the next ECG period. For periods that are longer than the average period, a portion of the original signal will not be represented in the composed matrix.

<u>Interpolation</u>

The sample duplication method creates the desired number of samples for each matrix row, but it does not isolate or preserve the shape of each individual ECG period. The following interpolation matrix alignment technique was implemented to remediate this:

1. Identify the number of samples in each RR period

2. Find the difference in samples between the average period and RR period (RR difference)

3. If the RR difference is zero, leave that segment alone and move on to the next period. If the RR difference is negative, the signal was downsampled by a factor of two equally from both sides of the middle of the RR period until the number of samples equaled the average period. If the RR difference is positive, adjacent pairs of samples near the middle of the RR period were used to linearly interpolate new samples until the number of samples equaled the average period. The middle of the period was used for interpolation because it minimizes the distortion of the ECG morphology as this region approaches zero and does not contain a P, QRS, or T wave.

Ensemble Empirical Mode Decomposition with Independent Component Analysis (EEMD-ICA)

Using the EEMD-ICA algorithm proposed by Mijovic *et al.*, we attempt to extract a non-stationary, spiky signal (fECG) from a combination of two spiky signals (mECG and fECG) and background noise, or an aECG. The aECG was preprocessed with the same notch and bidirectional Butterworth high pass filter used in the SVD extraction method. For EEMD, we randomized the np, determined the number of EMD iterations, and selected the optimal IMFs to

optimize ICA convergence. Preliminary tests proved that the convergence of ICA depended on

the np, which had an optimal value that changed with the SNR. To create a functional np for all

SNRs, the np was randomized between 0.2-2 [5] for every EMD iteration [13] . Similarly, the

number of EMD iterations affects ICA convergence. Modelling Liu's and Luan's fetal ECG

EEMD-ICA separation technique, we selected 200 iterations [14]. Finally, we modified the

number of IMFs input to ICA. Rather than averaging all ensemble IMFs, we selected the first

seven IMFs and discarded the IMFs that did not carry obvious fECG features. This selection was

based on a visual inspection of the IMFs and was consistent for all SNR. After the ICs were

calculated using ICA, we initially used visual inspection to determine a power threshold that

identified the IC that best represents the recovered fECG.

IV. Synthetic Signal Generation

To assess the accuracy of fECG extraction, SVD was performed on synthetic aECG. Synthetic ECG were used instead of real ECG to allow a point-to-point comparison of original and extracted fECG. The FECGSYN toolbox [15] was used to simulate 60 seconds of realistic aECG at a sampling frequency of 1 kHz and to generate the original R-peak location annotations for both the mECG and fECG. The aECG consisted of a prominent mECG, a weaker fECG, muscle artifact noise components, and a 50 Hz sine wave that simulates power line interference. All aECG signal components had maximum amplitudes in the 0-2 mV range. Different SNRs of the aECG were created as described in (3) and shown in Fig. 3 by holding the mECG and fECG constant and varying a noise multiplication factor (λ):

$$aECG = mECG + fECG + \lambda * (noise + 0.5 * sin(2 * pi * t)) \quad (3)$$

The parameter t in (3) is a 60 second array sampled at 1 kHz. The noise multiplication factor (λ) was changed to create fifteen SNRs ranging from -5.60 dB to -10.51 dB, where -5.60 dB contains the combined mECG and fECG without noise ($\lambda = 0$). The SNR was calculated as:

$$SNR = 10 \; x \; log_{10}(\frac{P(fECG)}{P(mECG + \lambda*(noise + 0.5*sin(2*pi*t)))}), where \; P(x) = power \; of \; x \quad (4)$$
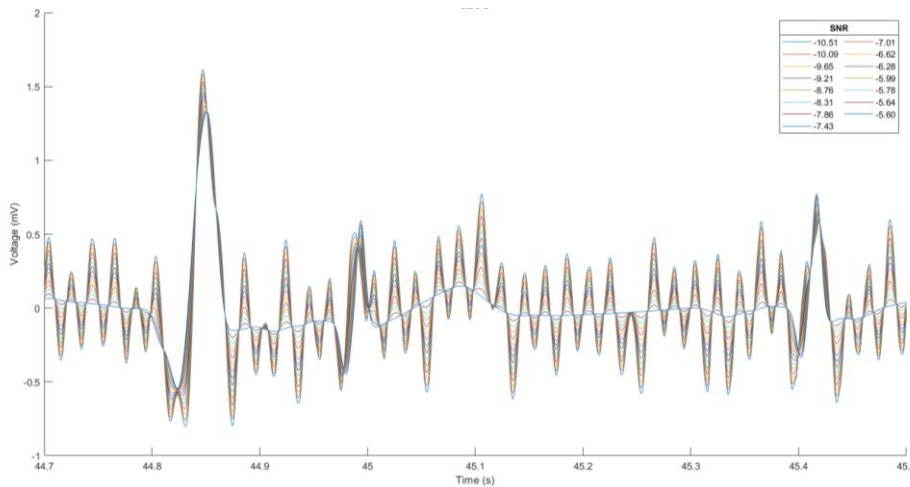

Fig. 3. One period of synthetic aECG at SNR ranging from -5.60 dB to -10.51 dB

V. Metrics

The quality of a fECG extraction algorithm is defined by its ability to reproduce the original fECG as well as the time required to perform the algorithm. A complex algorithm may perfectly construct fECG, but it often performs at a slow operation speed. In potential emergency settings, fast computation is necessary. However, a fast algorithm is also ineffective if it cannot produce necessary fECG characteristics. Both extraction quality and computational efficiency are important. Thus, the two fECG extraction methods of SVD and EEMD-ICA are compared across all SNRs using metrics that focus on extraction quality and computational efficiency.

Extraction Quality

Most fECG monitoring systems rely on fetal heart rate (fHR) to assess fetal health. However, fECG contains clinically important information embedded in its signal morphology as well [1]. To assess extraction quality of SVD, the output and input fECG were compared on R-peak detection accuracy and signal morphology.

A. R-Peak Detection Accuracy

R-peak detection accuracy relates to fHR in that the R-peak positions determine the fHR. If all R-peaks in the extracted fECG are properly preserved and identified, the extracted fHR should exactly match the original fHR. Variations in fHR can result from either improper fECG extraction or improper peak identification. The metrics used to assess R-peak detection accuracy include heart rate percent error (*HR % error*), sensitivity/precision (*SE*), positive predictive value/recall (*PPV*), and F1-score (*F1*), which are defined as:

$$HR \% \, error \; = \; \frac{abs(OrigHR - ExtHR)}{OrigHR} x100 \qquad (5)$$

$$SE \; = \; \frac{TP}{TP + FN} x \, 100 \qquad (6)$$

$$PPV = \frac{TP}{TP + FP} x\ 100 \qquad\qquad (7)$$

$$F1 = 2\ x\ \frac{TP}{2\ x\ TP + FP + FN} = \frac{2\ x\ PPV\ x\ SE}{100\ x\ (PPV + SE)} \qquad (8)$$

where *OrigHR* stands for original heart rate, *ExtHR* for extracted heart rate, *TP* for true positive,

FN for false negative, and *FP* for false positive. The *OrigHR* and *ExtHR* were calculated by

averaging RR periods. Locations of original R-peaks were supplied during synthetic signal

generation while extracted R-peaks were identified using the algorithm described in the SVD

implementation section. To identify the R-peaks as *TP*, *FP*, or *FN*, the locations of the extracted

and original R-peaks were compared. If the extracted R-peak was within a normal fetal QRS

duration of 40 milliseconds [16], the peak was accepted as a *TP*. Otherwise, the R-peak location

was marked as a *FP*. After complete analysis of the extracted R-peak locations, the remaining

uncompared, original R-peaks were marked as *FNs*. *SE* describes the percentage of correct peaks

from all original R-peaks, and *PPV* describes the percentage of correct peaks from all identified

peaks. Algorithms with high R-peak detection accuracy should have both high *SE* and high *PPV*.

F1 provides a metric to easily assess both *SE* and *PPV*. *F1* has a range of 0 to 1, where 0

represents *SE* and *PPV* scores of 0 percent and 1 represents *SE* and *PPV* scores of 100 percent.

B. Signal Morphology

Signal morphology of the extraction fECG was assessed in two ways: quantitatively and

qualitatively. Quantitatively, extracted fECG was compared on a point-to-point basis to the

original fECG using root mean square error (RMSE):

$$RMSE = \sqrt{\frac{1}{N}\sum_{i=1}^{N}|Orig(i) - Ext(i)|^2} \qquad\qquad (9)$$

where *Orig* is the original fECG and *Ext* is the extracted fECG. *RMSE* describes the distance the

extracted signal varies from the original signal. *RMSE* was only performed on EEMD-ICA for

reasons further discussed in sections VI.

In addition to quantitatively measuring fECG extraction with *RMSE*, qualitative assessment was performed by plotting the extracted fECG against the original fECG and original R-peak locations. This enabled overall morphology and noise removal comparison between SVD and EEMD-ICA.

Computational Efficiency

Computational efficiency measures the resources required by an algorithm. Common computational efficiency metrics include run-time, CPU usage, lines of code, and Big O notation. While run-time and CPU usage can provide useful information about system performance, these metrics are specific to the host system and programming platform. For example, a matrix-based program will likely run faster in MATLAB than in an ARM-based program. Likewise, increases in the number of CPU cores and RAM memory can significantly improve program run-time or CPU usage. Thus, run-time and CPU usage are not effective metrics for assessing algorithms that will be implemented on a variety of platforms. Similarly, lines of code is arbitrary to the programming language and programmer. For instance, a for loop can easily be written as multiple, longer if-statements.

Big O notation addresses the issue of arbitrary systems by estimating how run time grows as the input data size becomes infinitely large. In other words, Big O notation describes the worst case behavior of an algorithm. The best Big O of *O(1)* describes an algorithm that will operate at the same speed regardless of input data size. Big O becomes progressively more complex in the following sequence: *O(1)*, *O(log(n))*, *O(n)*, *O(nlog(n))*, $O(n^b)$, $O(b^n)$, *O(n!)*, where *n* is the input data size and *b* is an integer. Because of its adaptability, we use Big O notation to assess the computational efficiency of SVD and EEMD-ICA.

VI. Results

Extraction Quality

The extraction quality of SVD and EEMD-ICA were evaluated on the metrics discussed in section V. All results described in this section were based on extraction of the full-length 60 second synthetic aECGs. Because the EEMD-ICA fECG extraction varied with each iteration of the same SNR, the results from each method were averaged across 50 iterations [17].

A. F1

Both SVD and EEMD-ICA exhibited the expected increases in *F1* performance as SNR increased (Fig. 4). Across all SNRs, the *F1* values for both SVD methods were below one EEMD-ICA standard deviation. EEMD-ICA additionally maintained an average *F1* above 0.95 for SNRs greater than -10.08 dB while SVD only maintained a similar performance for SNRs above -8.75 dB. While EEMD-ICA's worst *F1* performance is 0.86, SVD with interpolation and sample duplication have minimum scores of 0.77 and 0.85, respectively. These results seem to indicate that overall EEMD-ICA is more successful at correctly identifying peaks.

However, EEMD-ICA becomes less reliable as the SNR decreases. At -10.51 dB, the standard deviation of EEMD-ICA increases from 0.015 or below to 0.083. Considering the maximum *F1* is 1, this means the EEMD-ICA *F1* at -10.51 dB can vary up to 8%. Additionally, there is only a difference of 0.0069 at -10.51 dB between EEMD-ICA and SVD with sample duplication. This is approximately eight times smaller than the difference of 0.0609 between two methods at -10.09 dB. This performance hit was paralleled by SVD with interpolation, so there may be a threshold at lower, unexplored SNRs where noise will greatly inhibit fECG extraction.
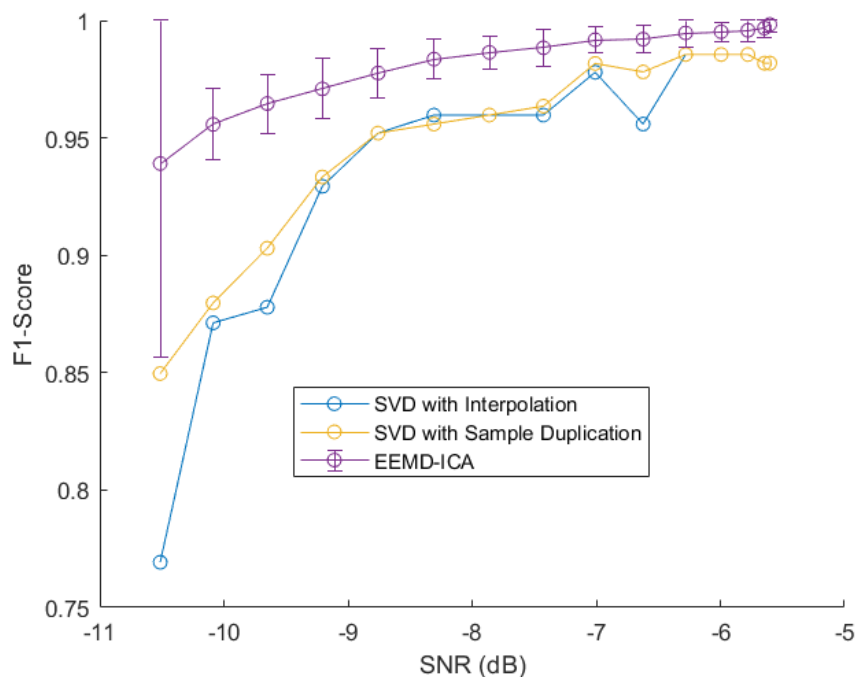
Fig. 4. F1-Score for fetal extraction techniques are SNR ranging from -5.60 dB to -10.51 dB

B. HR % error

All fetal extraction methods followed the expected trend of *HR % error* decreasing as SNR increased. Compared to both SVD methods, EEMD-ICA yielded lower *HR % error* within one standard deviation for all SNRs below -6.28 dB (Fig. 5). For SNRs -6.28 dB and above, the *HR % error*s of EEMD-ICA and both SVD methods were all below 0.11%. Overall, EEMD-ICA had lower *HR % error*s than both SVD methods; EEMD-ICA had a maximum error of 4.66% whereas SVD with interpolation and SVD with sample duplication had maximums of 13.30% and 7.90%, respectively. This trend agrees with the conclusion from the *F1* analysis that EEMD-ICA is more successful than SVD at correctly identifying peaks. The *HR % Error* also supports the previous conclusion that EEMD-ICA becomes less reliable at lower SNRs as the standard deviation increased from 0.56% at -10.09 dB to 3.4% at -10.51 dB. Finally, the *HR % error* of SVD with sample duplication was generally lower than the error of SVD with interpolation for

SNRs below -6.27 dB. The better performance of SVD with sample duplication is also reflected in the *F1* scores (Fig. 4), so it can be concluded that the matrix alignment techniques affect the performance of SVD.
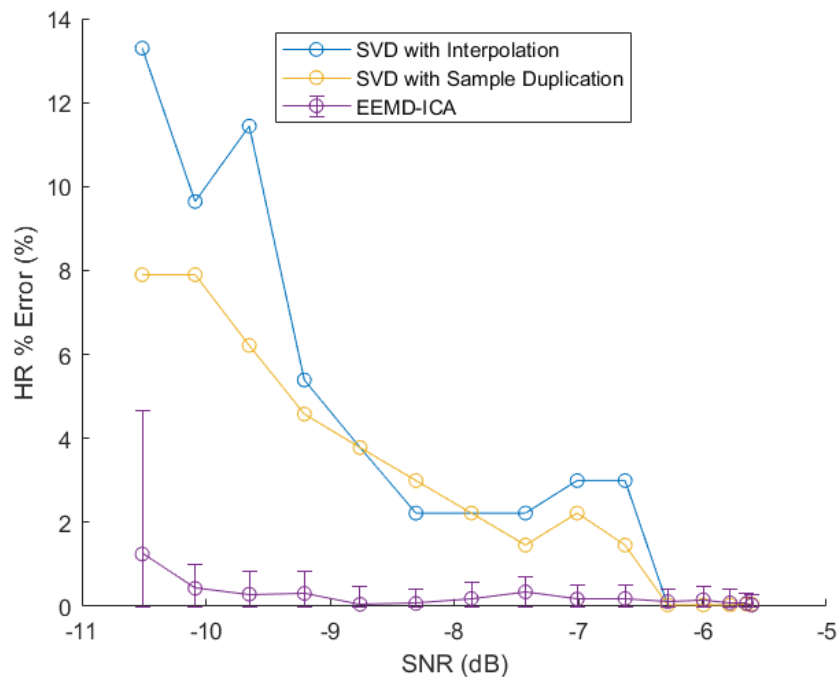

Fig. 5. HR % error for fetal extraction techniques at SNR ranging from -5.60 dB to -10.51 dB

C. SE/PPV

Similar to *HR % error* and *F1* score, both SVD and EEMD-ICA exhibited the expected increase in *SE* and *PPV* performance as SNR increased (Fig. 6). Across all SNRs, EEMD-ICA yielded a higher *SE* within one standard deviation than both SVD methods. Comparison of the two SVD methods showed that SVD with sample duplication generally possessed a higher *SE* but did not have a significantly higher *PPV* (Fig. 7) across SNRs below -6.27 dB. Because *SE* is a ratio of *TPs* to all expected R-peaks, this suggests that SVD with sample duplication identified true fetal R-peaks more consistently than SVD with interpolation. However, the fact that there is not a significant difference in *PPV*, which is the ratio of correct peaks out of all identified,

between the two SVD methods also suggests that SVD with sample duplication is also more prone to identifying false peaks (*FP*s).

*FP*s occur when expected R-peaks are shifted outside the 40 millisecond QRS proximity requirement or extra R-peaks are added. Further knowledge of *FP* peaks is required to determine which case is occurring. Presently, we are unable to determine without qualitative inspection how many of the *FP* peaks are also *FN* peaks. If the *FP* R-peaks are not *FNs*, the *PPV* performance is likely decreased by extra, falsely identified peaks. However if the *FP* peaks are also *FNs*, the lower *PPV* performance is the result of shifted, extracted peaks. If the *FP* of SVD with sample duplication is caused by the latter, this may result from the overlapping of ECG periods and could probably be fixed with better matrix alignment techniques.

Although the lower *SE* performance of SVD with interpolation does not confirm the prior statement, the method's results may be skewed by not carefully removing excess points in the matrix alignment technique. In some cases, it was found that dropping points in the maternal aECG component could result in the elimination of fetal R-peaks before the fECG was extracted. Preventing premature deletions of fetal peaks by improving the interpolation method should increase the number of peaks that can be identified as *TPs*, which could potentially improve all of the *PPV, SE*, and *F1* metrics.
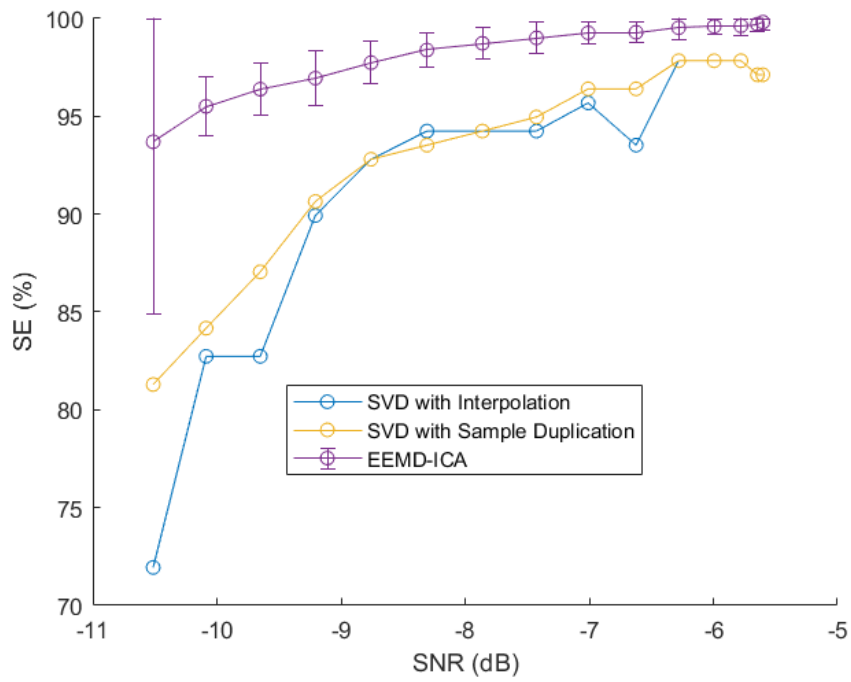
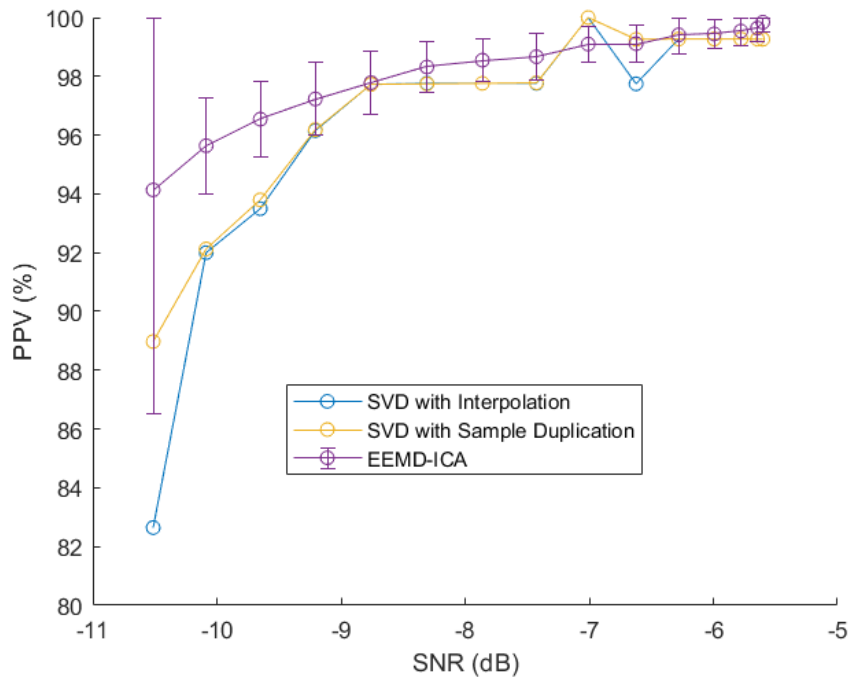*Fig. 6. SE for fetal extraction techniques at SNR ranging from -5.60 dB to -10.51 dB*

Fig. 7. PPV for fetal extraction techniques at SNR ranging from -5.60 dB to -10.51 dB

D. RMSE

  RMSE provides a method to quantitatively assess the signal morphology of the EEMD-ICA extraction method. *RMSE* could not be conducted on the SVD extraction methods because the size of the aECG signal was changed by downsampling and the matrix alignment techniques. The *RMSE* for EEMD-ICA followed the expected decreasing trend as the SNR increased (Fig. 8). While a maximum *RMSE* of 0.14 millivolts may seem insignificant, this value becomes significant when compared to the original fECG amplitudes. The maximum value of the original fECG is 0.79 millivolts. This means that the worst *RMSE* is at least 18% of the original fECG. As the amplitude decreases towards zero, the error approaches infinity. Overall, the *RMSE* of EEMD-ICA suggests the extracted signal contains a considerable amount of noise.
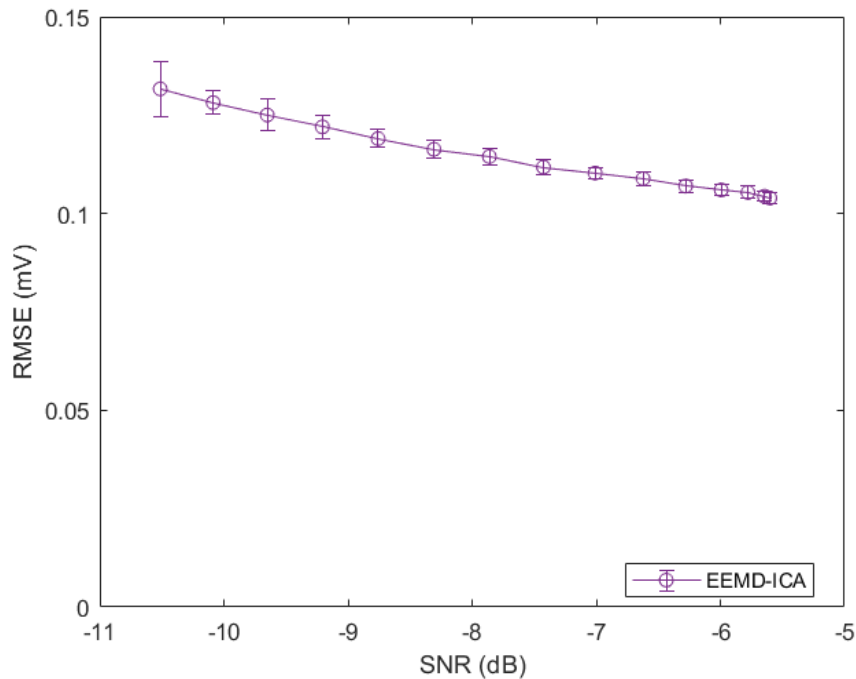

Fig. 8. RMSE of EEMD-ICA at SNR ranging from -5.60 dB to -10.51 dB

E. Signal Morphology

Because the SVD extraction method could not be quantitatively compared to the original signal using *RMSE*, a qualitative comparison was performed. Six periods of the extracted fECG from the three extraction methods were compared to the original fECG at a SNR of -7.01 dB from 2 to 4.5 seconds (Fig. 9). The two SVD methods are displayed by a single signal because they could not be distinguished as different for this segment by the naked eye. The SVD methods become more distinguishable as the SNR decreases. Compared to both SVD methods, EEMD-ICA contained more noise as well as prominent maternal artifacts at 2.12, 2.86, 3.63, and 4.38 seconds. The excess noise present in the EEMD-ICA extracted fECG obscured all fECG components (i.e. P- or T-waves) except the QRS complex. In contrast, both SVD extracted fECG contained a limited amount of noise, and part of the P-wave as well as the QRS complex were preserved. This component preservation means that SVD is currently the best method for extracting fECG with minimal noise.
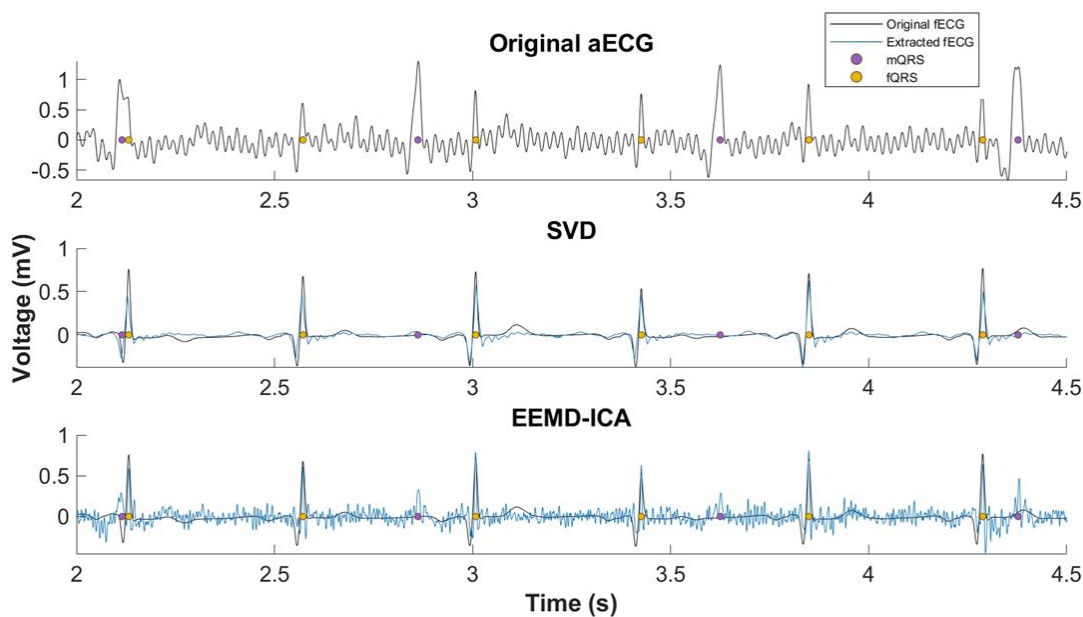

Fig. 9. Qualitative comparison of extracted to original fetal signals at SNR of -7.01 dB

Computational Efficiency

The comparison of Big O notation was performed by assuming each extraction technique processed the same amount of data: the input aECG was assumed to be an mxn input aECG matrix, where $n >> m$. It was assumed that SVD and EEMD-ICA were the most demanding parts of each algorithm and represented the complexity of the entire fetal extraction process. The complexity of SVD and EEMD-ICA are $O(mn^2+n^3)$ [4] and $O(nlog(n)+m^2n)$, respectively [18, 19]. Comparing the two Big O notations, the mn^2 and n^3 terms for SVD grow at faster rates than the m^2n and $nlog(n)$ terms for EEMD-ICA, respectively. Thus, SVD is more complex than EEMD-ICA.

Although Big O notation suggests that EEMD-ICA is more computationally efficient than SVD, the observed runtimes did not coincide with this finding. For every SNR of the supplied aECG, a significantly longer runtime was observed for EEMD-ICA than SVD. This highlights the limitations of utilizing Big O as a metric for computational efficiency. The assumption that SVD and EEMD-ICA encompass the majority of the complexity ignores the complexity of other design elements. In the case of SVD, it is important to note that downsampling, preprocessing, and interpolating are not accounted for within the Big O calculations. The downsampling of the input aECG reduces the method complexity by a factor of eight. Thus, SVD can still be more computationally efficient than EEMD-ICA with the same dataset. In contrast, the Big O complexity of EEMD-ICA will be increased by considering the number of EEMD iterations and the ICA convergence variations. Thus, the design complexity of other algorithm components for both SVD and EEMD-ICA explains the discrepancy between the observed runtime and the calculated Big O.

VII. Real Signal Application

To further assess the extraction quality of SVD and EEMD-ICA, the extraction techniques were applied to a real aECG. More specifically, the real aECG is channel 3 from record a25 of the 2013 PhysioNet Computing in Cardiology Noninvasive Fetal ECG Database [11]. Fig. 10 displays the results of a qualitative analysis on the extracted signals.
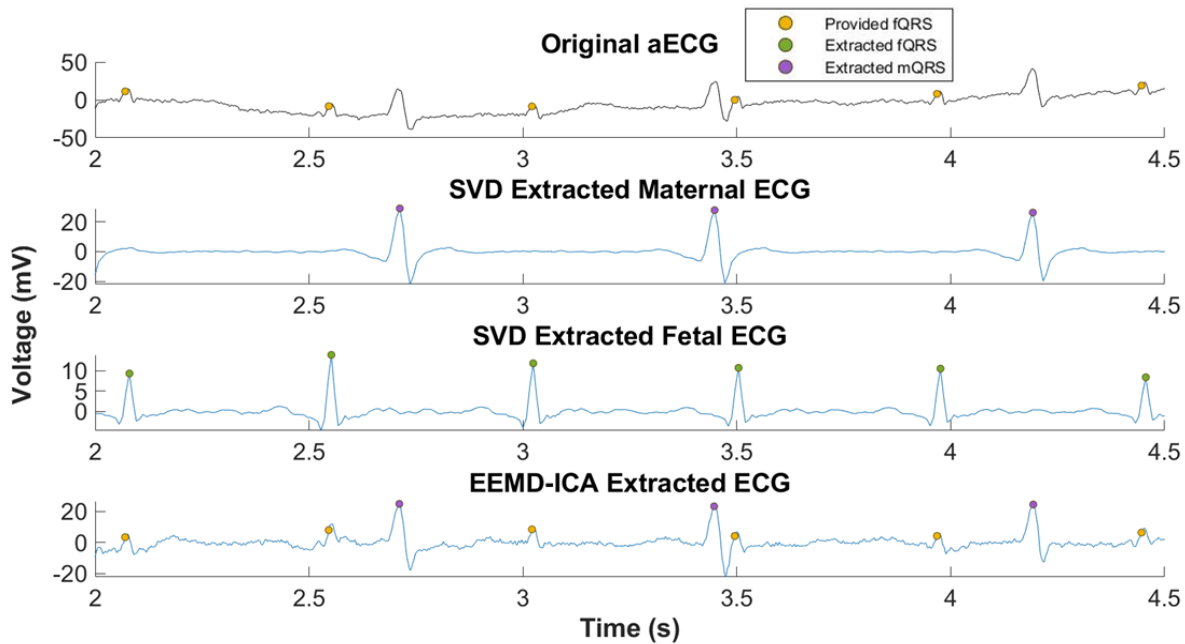

Fig. 10. Qualitative comparison of extracted to original ECG on real aECG

The original aECG and EEMD-ICA plots in Fig. 10 notate the expected fetal QRS complexes (fQRS) using the locations provided by PhysioNet. All other notated QRS peaks were determined using the peak location algorithm discussed in section III. As discussed with Fig. 9 of section VI, a single signal is used to represent both SVD extraction techniques because the results are not noticeably different.

The two SVD extractions show clean recovery of the mECG and fECG components with accurate peak locations. This recovery resembles the results produced by applying SVD to the synthetic signal. In contrast, our implementation of EEMD-ICA did not demonstrate the ability

to extract the fetal signal when applied to a real signal. Rather, EEMD-ICA denoised the original aECG, and the peak detection algorithm was only able to identify the maternal peaks. Because EEMD-ICA performed well at identifying fetal peaks on the synthetic signal, this may suggest that more preprocessing is required for EEMD-ICA to extract the fECG. Overall, SVD was found to produce better extraction of the mECG and fECG components on real aECG.

VIII. Discussion

The quantitative results of *F1*-score, *PPV*, *SE*, and *HR % error* from the synthetic signal

tests demonstrate that EEMD-ICA has the ability to consistently perform better than both SVD

techniques at R-peak identification. Despite the high precision in peak identification on the

synthetic signal, qualitative analysis of the synthetic and real fECG extraction exhibits the

inability of our EEMD-ICA implementation to completely extract the fECG without mECG or

noise components. In contrast, both SVD methods offered clean fECG morphology extraction for

both the synthetic and real aECG. Although SVD may not have performed as well as EEMD-

ICA at R-peak identification, we demonstrated through an analysis of *SE*, *PPV*, and *FPs* that the

precision of SVD in R-peak identification might improve with modifications to the matrix

alignment technique. Additionally, the longer observed runtime and instability of convergence

variations at lower SNRs for EEMD-ICA make it less favorable than SVD for future

applications. However, further investigation of different matrix alignment techniques to improve

R-peak detection is necessary for SVD to be accepted as a fetal ECG extraction technique in the

medical community.

IX. Conclusions

Extracting the fECG from the aECG of a pregnant mother can help monitor the cardiovascular health of the fetus. In this work**,** we implemented and compared variations of Kanjilal *et al.*'s SVD and Mijovic *et al.*'s EEMD-ICA single-channel fECG extraction methods on their extraction quality and computational complexity. Our results show that when comparing extraction quality on a synthetic aECG, EEMD-ICA succeeds at detecting R-peaks while SVD better maintains fECG morphology. This result was not replicated when SVD and EEMD-ICA were applied to a real aECG from a PhysioNet Noninvasive Fetal ECG Database. Despite a lower computational efficiency, EEMD-ICA possessed a longer runtime due to unaccounted complexity of design within Big O notation. In addition to confirming the potential for each extraction method, we highlight areas of improvement for each method. For SVD, we suggest improving the matrix alignment technique. For EEMD-ICA, we suggest improving the noise and mECG component extractions by applying more preprocessing to the aECG. Finally, refinement of the peak locating algorithm would benefit both fECG extraction methods.

Although the current method implementations only partially extract the fECG correctly, we expect that future work building on our methodology will vastly improve the methods' extractions and comparison. For example, quantifying SVD morphology through RMSE would allow for direct comparison between SVD and EEMD-ICA. Additionally, future work can expand the dataset to include more SNRs, different synthetic base signals, and real ECG signals. Testing the results on more SNRs can provide insight into the impact different matrix alignment techniques have on SVD. Furthermore, testing more synthetic and real signals can validate the current results and the potential of single-channel fECG extraction for future medical devices.

References

[1]   M. A. Hasan, M. Reaz, M. Ibrahimy, M. Hussain, J. Uddin, "Detection and Processing Techniques of FECG Signal for Fetal Monitoring," *Biological procedures online*, vol. 11, pp. 263-95, Mar. 2009.

[2]   B. Widrow, J. M. McCool, J. Kanmitz, C. Williams, R. Hearn, J. Zeidler, E. Dong, and R. Goodlin, "Adaptive noise cancelling: Principles and applications," *Proc. IEEE*, 1975, vol. 63, no. 12, pp. 1692-1716.

[3]   T. Kawakita, U. M. Reddy, H. J. Landy, S. N. Iqbal, C. Huang, K. L. Grantz, "Neonatal complications associated with use of fetal scalp electrode: a retrospective study," *BJOG*, 2016, vol. 123, no. 11, pp. 1797-1803.

[4]   P. P. Kanjilal, S. Palit, G. Saha, "Fetal ECG extraction from single-channel maternal ECG using singular value decomposition," *IEEE Trans. on Biomed. Eng.*, vol 44, no. 1, pp. 51-59, Jan. 1997.

[5]   B. Mijović, M. De Vos, I. Gligorijevic, J. Taelman, S. Van Huffel, "Source Separation From Single-Channel Recordings by Combining Empirical-Mode Decomposition and Independent Component Analysis," *IEEE Trans. Biomed. Eng.*, vol. 57, no. 9, pp. 2188-2196, Sep. 2010.

[6]   P. Flandrin and P. Goncalves, "Empirical mode decomposition as data driven wavelet-like expansion," *Int. J. Wavel., Multires. Inf. Proc.*, vol. 2, no. 4, pp. 477–496, 2004.

[7]   N.E. Huang et al., "A confidence limit for the empirical mode decomposition and Hilbert spectral analysis," *Proc. R. Soc. London. A.*, vol. 459, no. 2037, pp. 2317–2345, Sep. 2003.

[8]   W. Zhaohua and N. E. Huang, "Ensemble empirical mode decomposition: a noise assisted data analysis methods," *Advances in Adaptive Data Analysis.*, vol. 24, no. 1, pp. 1–41, 2009.

[9]   G.D Clifford, "Singular Value Decomposition & Independent Component Analysis for Blind Source Separation," 2005, unpublished.

[10]   A. Hyvärinen, "Fast and robust fixed-point algorithm for independent component analysis", *IEEE Transactions on Neural Networks*, vol. 10, no. 3, pp. 626-634, 1999.

[11]   A. Goldberger et al. "PhysioBank, PhysioToolkit, and PhysioNet: components of new research resource for complex physiological signals," *Circulation*, vol. 101, no. 23, pp. 215-220, 2003.

[12]   G. Lamesgin, Y. Kassaw, D. Assefa, "Extraction of fetal ECG from abdominal ECG and heart rate variability analysis," Advances in Intelligent Systems and Computing, vol 334, pp. 65-75, 2015.

[13]   J. Leng, S. Jing, C. Luao, Z. Wang, "EEMD-Based cICA method for single-channel signal separation and fault feature extraction of gearbox", Journal of Vibroengineering, vol. 19, no. 8, pp. 5858-5873, 2017.

[14]   G. Liu and Y. Luan, "An adaptive integrated algorithm for noninvasive fetal ECG

separation and noise reduction based on ICA-EEMD-WS," *Med Biol Eng Comput*, vol.

53, no. 11, pp. 1113–1127, Nov. 2015, doi: 10.1007/s11517-015-1389-1.

[15]   F. Andreotti, J. Behar, S. Zaunseder, J. Oster, G. D. Clifford, "An Open-Source

Framework for Stress-Testing Non-Invasive Foetal ECG Extraction Algorithms,"

Physiol. Meas., vol. 37, no. 5, pp. 627-648, Apr. 2016.

[16]   K. M. J. Verdurmen *et al.*, "Normal ranges for fetal electrocardiogram values for the

healthy fetus of 18–24 weeks of gestation: a prospective cohort study," *BMC Pregnancy

and Childbirth*, vol. 16, no. 1, p. 227, Aug. 2016.

[17]   K. Zeng, D. Chen, G. Ouyang, L. Wang, X. Liu, and X. Li, "An EEMD-ICA Approach to

Enhancing Artifact Rejection for Noisy Multivariate Neural Data," *IEEE Transactions on

Neural Systems and Rehabilitation Engineering*, vol. 24, no. 6, pp. 630–638, Jun. 2016,

doi: 10.1109/TNSRE.2015.2496334.

[18]   V. Laparra, G. Camps-Valls, J. Malo, "Iterative Gaussianization: From ICA to Random

Rotations," *IEEE Trans. on Neural Networks*, vol. 22, no. 4, pp. 537-549, Apr. 2011.

[19]   Y. Wang, C. Yeh, H. V. Young, K. Hu, M. Lo, "On the computational complexity of the

empirical mode decomposition algorithm," *Physica A: Statistical Mechanics and its

Applications*, vol. 400, pp. 159-167, Apr. 2014.

Appendices

A. Previous Research Versions

The initial version of this research was conducted at University of Washington Bothell (UWB) during the summer of 2019 in correspondence with University of Florida undergraduate Koen Flores and UWB advisor Dr. Tadesse Ghirmai. The initial version was additionally presented at the 2019 Annual BMES Meeting as an undergraduate poster under the name "Comparative Study of Single-Lead Fetal ECG Extraction Methods." This research differed from the current version in that the extraction methods were not applied to a real aECG, 20 (instead of 50) trials were performed, power line interference was not simulated in the synthetic aECG, fewer SNRs were tested, and the peak location algorithm did not adapt the number of expected peaks to the type of ECG analyzed. Rather, only one peak was required to be found regardless of ECG type. The findings from the initial version of the research are consistent with the current results but updating the peak location algorithm to consider ECG type greatly improved the results of *F1*-score, *HR % Error*, and *SE* for all extraction methods.

B. Individual Contributions

In the initial version of the research, Elizabeth Staley and Koen Flores collaborated to implement and analyze the fECG extraction techniques. The work was roughly separated as detailed below. All modifications to the initial research were completed by Elizabeth Staley and are *italicized*.

Koen
- Wrote preprocessing code
- Formed the matrix required for SVD
- Created the SVD interpolation technique
- Developed EEMD code

- Analyzed and integrated FastICA code

- Designed the graphics shown in Fig. 1 and Fig. 2

- Manually performed EEMD-ICA result analysis

- Plotted all results in EXCEL

Elizabeth

- Wrote file to validate the contents of and convert a CSV file of aECG to a matrix

- Generated the synthetic aECG

- Produced the peak location code

- Designed IC selection code for EEMD-ICA

- Developed metrics code

- Coordinated function calls in main file

- Created batch script to automatically run tests of all SNRs

- *Regenerated synthetic signals to contain power line interference and have more SNRs*

- *Updated the peak location code to consider the type of ECG*

- *Applied SVD and EEMD-ICA to a real aECG from the 2013 PhysioNet Computing in Cardiology Noninvasive Fetal ECG Database*

- *Modified the batch script to easily calculate the mean and standard deviation of 50 EEMD-ICA trials*

- *Moved plotting from EXCEL to MATLAB*

Honors Thesis - Elizabeth Staley

Emil Jovanov <emil.jovanov@uah.edu>   Wed, May 6, 2020 at 9:42 PM
To: Elizabeth Staley <eds0017@uah.edu>
Cc: Ravi Gorur <rsg0004@uah.edu>, William Wilkerson <wilkerw@uah.edu>, David Cook <dac0010@uah.edu>

Dear all,
please find attached Honor's Thesis of Elizabeth Staley
with our signatures.
Please let me know if you have any questions
or need anything else.

Best regards

Emil.

--
Dr. Emil Jovanov.
Electrical and Computer Engineering Dept
The University of Alabama in Huntsville
http://www.ece.uah.edu/~jovanov
Phone (256) 824 5094

📄 **Staley_HON_Capstone_EJ.pdf**
906K